

THIN FILM FLOW ON AN INCLINED CHANNEL

Leo Hari Wiryanto[✉]^{1*}, Sudi Mungkasi[✉]², Ikha Magdalena[✉]³

^{1,3} Faculty of Mathematics and Natural Sciences, Institut Teknologi Bandung
Jln. Ganesha 10, Bandung, 40132, Indonesia

²Department of Mathematics, Faculty of Science and Technology, Sanata Dharma University
Jln. Affandi, Mrican, Caturtunggal, Depok, Sleman, Yogyakarta, 55281, Indonesia

Corresponding author's e-mail: * lhw@itb.ac.id

Article Info

Article History:

Received: 4th August 2025

Revised: 6th January 2026

Accepted: 8th March 2026

Available online: 8th April 2026

Keywords:

Finite difference method;

Lubrication theory;

Single equation;

Thin film flow.

ABSTRACT

A two-dimensional fluid is considered on an inclined channel. The depth of the fluid is small, so that it can be modeled as a single equation of the fluid depth, from the lubrication theory. The model is then solved numerically by an implicit finite difference method, to observe the surface wave propagation from the parameters such as the inclination of the channel and the ratio of the fluid thickness with respect to the wavelength. The effect of non-linearity of the model indicates that the wave propagates with changing the form, decreasing the amplitude, and tending to an almost shock wave. Those are simulated in this paper.



This article is an open access article distributed under the terms and conditions of the [Creative Commons Attribution-ShareAlike 4.0 International License](https://creativecommons.org/licenses/by-sa/4.0/).

How to cite this article:

L.H. Wiryanto, S. Mungkasi, and I. Magdalena, "THIN FILM FLOW ON AN INCLINED CHANNEL," *BAREKENG: J. Math. & App.*, vol. 20, no. 3, pp. 2151-2162, Sep. 2026.

Copyright © 2026 Author(s)

Journal homepage: <https://ojs3.unpatti.ac.id/index.php/barekeng/>

Journal e-mail: barekeng.math@yahoo.com; barekeng_journal@mail.unpatti.ac.id

Research Article · Open Access

1. INTRODUCTION

A two-dimensional fluid flowing on an inclined channel is considered. Most of the work for that problem is usually modelled in shallow water equations. We can read such as in Wiryanto [1], Budiasih and Wiryanto [2], and Fauzi and Wiryanto [3]. When the flow is disturbed by a bump, the flow generates surface waves, such as studied by Wiryanto and Jamhuri [4], Magdalena and Wiryanto [5]. The model of shallow water equations is derived based on the moderate thickness of the fluid. In contrast, when the thickness is very-very small, the governing equation can be simplified from Navier-Stokes into the theory of lubrication. This derivation can be seen, for example, in Van Dyke [6], Acheson [7], and Pozrikidis [8]. That theory was also applied by King et al. [9] for modeling a steady thin viscous flow with air-blown above the fluid. Oron and Rosenau [10] reported their work on a film flowing down the underside of an inclined plate, which is called negative gravity. Abdalall et al. [11] studied the travelling waves as a result of numerical and experimental models. Some applications of thin film flow have been studied widely, for example, in Kalliandasis et al. [12]. Meanwhile, Wiryanto and Febrianti [13] formulated the thin film flow from the theory of lubrication into a single non-linear equation of the fluid depth, in the unsteady case. Since the nonlinearity of the equation, Wiryanto and Febrianti [13] solved the model numerically by introducing forward time central space. The method was an explicit finite difference, which was conditionally stable. This is an obstacle in expanding observations, especially in discretizing the numerical domain, involving the physical quantities such as the viscosity and density. Another numerical approach has been done by Wiryanto [14], [15] to analyze the stability. Those are then applied by Wiryanto et al. [16] to make the simulation of wave propagation. They are restricted to the simulation as a condition of the numerical method.

Recently, Putra et al. [17] developed an implicit method applied to the linearized equation of the thin film model. Forward-time central-average-space was applied to the linearized equation to construct a system of linear equations, and then Gauss-Seidel iteration was used to solve the equations. This method was also analyzed for stability, and they found that it is unconditionally stable. This implicit method confirms the results obtained in [13], and can be used for a larger step size of time. Wiryanto and Djohan [18] then developed the implicit method for the linear model by involving surface tension. The success of the implicit method opens the opportunity to apply it to the nonlinear equation. Some works relating to developing the implicit method can be seen in Wiryanto and Achirul [19] and Wiryanto [20], [21] for solving the Korteweg de Vries (KdV) equation as the model for various waves. The discretization of the non-linear term is approximated by a Taylor polynomial, and then used forward-time central-average-space. This step was not done in [17], as the equation was already linear.

The numerical procedure proposed above can solve the thin film non-linear equation. Simulation is then presented in this paper as a two-parameter family solution. The two parameters are the inclination and the ratio between the fluid depth and the wavelength. Physically, the second parameter corresponds to the wave speed, as the effect of the scaling of time.

The scaling process is often used in numerical procedures. It is determined according to the purpose of the observation. Rohlf's and Pischke [22], for example, introduce the scaling process in thin film flow based on Reynolds numbers, Kapitza number, and the inclination of the channel to see the domination of forces in the model. Meanwhile, the equation solved in this paper is scaled to observe that the wave propagation was originally so slow, and the wave elevation was much smaller compared to the wavelength. The improvement of the calculation is in balancing the coefficient of each term in the equation. Therefore, the scaling variables are required, and the equation is able to present the wave evolution with almost no shock for an initial wave satisfying a certain condition. Analytically, we derive that condition. Our result for shock wave similar to King et al. [9] for steady case, and some other works for model of shallow water equation such as Fauzi and Wiryanto [23], [24], Needham and Merkin [25], Merkin and Needham [26], far long before Dressler [27] formulated shock wave analytically, called as roll-waves.

2. RESEARCH METHOD

In this section, we provide the problem formulation and the numerical procedure to solve the mathematical equation of the problem. This section is an extension of the works of Wiryanto and Febrianti [13], Wiryanto and Achirul [19], as well as Wiryanto [20], [21].

2.1 Problem Formulation

The derivation of thin film flow on an inclined channel can be seen in Wiryanto and Febrianti [13]. The fluid thickness is h measured from the bottom channel, inclined at an angle θ . The effect of gravity, the fluid of density ρ and viscosity μ appears in the following equation, Eq. (1),

$$h_t + \frac{\rho}{3\mu} [h^3 \{-h_x g \cos \theta + g \sin \theta\}]_x = 0. \quad (1)$$

We choose the coordinate x along the bottom of the channel. t represents the variable of time. Wiryanto and Febrianti [13] derived Eq. (1) based on the lubrication theory, subject to bottom and surface conditions.

To reduce the number of physical parameters, we prefer to work on scaling variables by introducing

$$\bar{x} = \frac{x}{L}, \quad \bar{h} = \frac{h}{h_0}, \quad \bar{t} = \frac{t}{\tau},$$

where L is wavelength, h_0 is a small constant solution and $\tau = \frac{3\mu L}{\rho g h_0^2}$. So that, when we apply that scaling to Eq. (1), we obtain an equation, written without a bar.

$$h_t + a(h^3)_x + b(h^4)_{xx} = 0, \quad (2)$$

where $a = \sin \theta$ and $b = -\frac{1}{4}r \cos \theta$. We use notation $r = h_0/L$. This new notation (written without a bar) in Eq. (2), after scaling, is necessary to avoid ambiguity.

By using that scaling, the new variables above physically compress the waves from wave-length L to smaller, and also to reduce the observation time. Therefore, that process is expressed by the scaling quantities r and τ . For small r , it affects \bar{t} , that is proportional to r multiplied by t . So, the unity of \bar{t} means very large in the value of t . Therefore, the numerical solution in [13] could not obtain the shock wave, a similar result in [28] and [29]. Otherwise, it was required for much longer calculations and a long observation domain. The scaling process has been introduced by many researchers.

In case $b = 0$, Eq. (2) followed by the initial condition $h(x, 0) = f(x)$ has a solution in implicit form

$$h(x, t) = f(x - 3a h^2 t), \quad (3)$$

see, for example, in Strauss [30]. The surface of the fluid can form a shock wave, predicted in an interval x giving $f'(x) < 0$. Suppose $x \in (\alpha, \beta)$ then at position $x = \gamma$ a discontinuity in h will occurs. The value of γ can be determined by integrating Eq. (2), without involving the third term

$$\partial_t \int_{\alpha}^{\beta} h(\xi, t) d\xi + a[h^3(\beta, t) - h^3(\alpha, t)] = 0.$$

Since h is smooth except at $x = \gamma$, possible depends on t , the integral splits into two, and differentiate with respect to t , we obtain

$$\left[h^-(\gamma(t), t) \gamma_t + \int_{\alpha}^{\gamma} h_t(\xi, t) d\xi \right] - h^+(\gamma(t), t) \gamma_t + \int_{\gamma}^{\beta} h_t(\xi, t) d\xi + a[h^3(\beta, t) - h^3(\alpha, t)] = 0.$$

Here we denote h^- as the limit value of h evaluated $x \rightarrow \gamma$ from the left. Similarly, for h^+ , evaluated from the right. The next step is to replace h_t by $-a(h^3)_x$ in the integrand, so that the result of the integral can be used to cancel $h^3(\alpha, t)$ and $h^3(\beta, t)$. After some algebraic operations, we obtain

$$\gamma_t = a((h^-)^2 + h^- h^+ + (h^+)^2). \quad (4)$$

This analysis will be compared to our numerical solution.

2.2 Numerical Procedure

In this sub-section, we describe the numerical procedure for Eq. (2). The first step is to discretize the observation domain by a homogeneous sub-domain with length dx and we write each point of the sub-domain $x_i = i dx$, $i = 0, 2, \dots, I$, and step size for time dt so that we denote $t_n = n dt$, $n = 0, 1, 2, \dots$. The value of h at x_i and t_n denoted by $h_i^n \approx h(x_i, t_n)$.

Following Wiryanto and Achirul [19], and Wiryanto [20], [21], we write the second term in Eq. (2), i.e. $g(h) = h^3$, and the discretizing of g_x is approximated by the average central space

$$g_x \approx \frac{1}{2} \left\{ \frac{g_{i+1}^{n+1} - g_{i-1}^{n+1}}{2 dx} + \frac{g_{i+1}^n - g_{i-1}^n}{2 dx} \right\} \\ = \frac{g_{i+1}^{n+1} + g_{i+1}^n - (g_{i-1}^{n+1} - g_{i-1}^n)}{4 dx}.$$

Meanwhile, the value of g at t_{n+1} is approximated by the first-order Taylor polynomial

$$g_i^{n+1} \approx g_i^n + \frac{\partial g}{\partial t} dt,$$

then express g_t in h and discretize in h_i^n so that we obtain

$$g_i^{n+1} \approx 3(h_i^n)^2 h_i^{n+1} - 2(h_i^n)^3.$$

From those, the discretization of g_x can be written in h_i^n

$$g_x \approx \frac{1}{4 dx} [3(h_{i+1}^n)^2 h_{i+1}^{n+1} - (h_{i+1}^n)^3 - (3(h_{i-1}^n)^2 h_{i-1}^{n+1} - (h_{i-1}^n)^3)].$$

Similarly, the third term in Eq. (2), we write $s(h) = h^4$, and the second derivative

$$s_{xx} \approx \frac{1}{2 dx^2} [s_{i+1}^{n+1} + s_{i+1}^n - 2(s_i^{n+1} + s_i^n) + (s_{i-1}^{n+1} + s_{i-1}^n)].$$

This is then expressed in h_i^n

$$s_{xx} \approx \frac{1}{2 dx^2} [4(h_{i+1}^n)^3 h_{i+1}^{n+1} - 2(h_{i+1}^n)^4 - 2(4(h_i^n)^3 h_i^{n+1} - 2(h_i^n)^4) + (4(h_{i-1}^n)^3 h_{i-1}^{n+1} - 2(h_{i-1}^n)^4)].$$

The next step is to discretize Eq. (2) by using the result above for g_x and s_{xx} , followed by forward time for h_t . After rearranging the finite difference equation into an implicit form of h^{n+1} , we obtain a system of linear equations

$$Ah_{i+1}^{n+1} + Bh_i^{n+1} + Ch_{i-1}^{n+1} = R, \quad (5)$$

where

$$\begin{cases} A = \frac{3a}{4 dx} (h_{i+1}^n)^2 + \frac{4b}{2 dx^2} (h_{i+1}^n)^3, \\ B = \frac{1}{dt} - \frac{4b}{dx^2} (h_i^n)^3, \\ C = -\frac{3a}{4 dx} (h_{i-1}^n)^2 + \frac{4b}{2 dx^2} (h_{i-1}^n)^3, \\ R = ah_{i+1}^n + \beta h_i^n + \delta h_{i-1}^n, \end{cases}$$

and the coefficients in R :

$$\alpha = \frac{a}{4 dx} (h_{i+1}^n)^2 + \frac{b}{dx^2} (h_{i+1}^n)^3, \\ \beta = \frac{1}{dt} - \frac{2b}{dx^2} (h_i^n)^3, \\ \delta = -\frac{a}{4 dx} (h_{i-1}^n)^2 + \frac{b}{dx^2} (h_{i-1}^n)^3.$$

We evaluate h at level time $n + 1$ simultaneously for $i = 1, 2, \dots, I$ using the values h at level n , and the left and right boundaries h_0^{n+1} and h_{I+1}^{n+1} . The system in Eq. (5) can be solved using any solver for systems of linear equations, and in this paper, we solve it iteratively using the Gauss-Seidel method. In the programming implementation, our numerical simulations start with specifying all parameter values, setting initial and boundary conditions, discretising the space and time domains, and evolving the numerical scheme Eq. (5) iteratively for all spatial points at each temporal point.

3. RESULTS AND DISCUSSION

The numerical procedure described above is used to solve Eq. (2), followed by the initial condition h_i^0 and for various values of the parameters θ and r . Most of our calculations use $dx = 0.1$, $dt = 0.1$, and the iteration error for the Gauss-Seidel method $\epsilon = 10^{-6}$. The spatial step and time step values are chosen for stability, based on the analysis for the linear problem, as in [17] and [18]. A necessary condition for the stability of the method is that the time step must satisfy the Courant-Friedrichs-Lewy (CFL) condition. This CFL condition makes the physical domain of dependence the same as the numerical domain of dependence. Considering this CFL condition, we take the time step small enough such that we obtain stable numerical solutions. All numerical computations are done in the Fortran programming language, and the results are plotted using MATLAB software on a laptop with a Windows operating system.

First, we make an animation of wave propagation $h(x, t)$ as the solution of Eq. (2) for the case $\theta = 0.087$ radian or $\sim 5^\circ$ and $r = 0$, case $b = 0$ to show that shock occurs at $x = \gamma$ as formulated in Eq. (4). The initial value is

$$h(x, 0) = f(x) = \begin{cases} 1.5, & \text{for } 0 < x \leq 30, \\ 1.5 - 0.025(x - 30), & \text{for } 30 < x < 50, \\ 1, & \text{for } 50 \leq x < 100. \end{cases} \quad (6)$$

As described in the previous section, $f'(x) = -0.025$ for $30 < x < 50$, a shock wave would occur. We confirm this by our numerical solution, as shown in Fig. 1 (a). There is a small interval of x giving h becomes sharper and sharper, together with reducing the interval. When we continue our calculations, the interval tends to a point with a discontinuity for h , that is what we call a shock wave. Our calculation should be stopped before that shock wave occurs, as it would be possible to have two values of h at the same position x , and the numerical procedure is not designed for that case. Moreover, in that animation, we can observe small waves appearing at the crest of the surface, i.e, near a sharp area. The position of shock can be calculated by Eq. (4), giving $\gamma_t = 0.41325$, and using $\gamma(0) = 40$ as the midpoint of the interval where $f'(x) < 0$, we obtain $\gamma(60) = 64.795$. This agrees with our numerical calculation. We then repeat the calculation using $r \neq 0$ but relatively small, we use $r = 0.002$. Similar plot in Fig. 1, we obtain with a slower wave speed, a front wave with a slope less than zero is still obtained until calculation up to $t = 200$. The form with almost shock can be obtained for longer calculations.

Now, we use a different initial wave

$$h(x, 0) = f(x) = \begin{cases} 1.0, & \text{for } 0 < x \leq 30, \\ 1.0 + 0.025(x - 30), & \text{for } 30 < x < 50, \\ 1.5, & \text{for } 50 \leq x < 100, \end{cases} \quad (7)$$

for $\theta = 5^\circ$ and $r = 0$. In contrast with the previous initial wave, we have $f'(x) = 0.025 > 0$ for $30 < x < 50$, and this would not cause a shock wave. We present in Fig. 1 (b). The area where the value $h > 0$ increases with time. Therefore, our numerical solutions confirm our analysis presented in the previous section.

In Fig. 2 (a), we show the animation of waves propagating on the surface of a thin film satisfying Eq. (2). We plot our calculation for some values of t , by shifting t from zero to $t = 500$. This is calculated using $\theta = 5^\circ$ and $r = 0.002$. As the initial wave is

$$h(x, 0) = 1 + 0.1 \sin\left(\frac{\pi x}{25}\right), \quad (8)$$

followed by the boundary condition

$$h(x, t) = 1 + 0.1 \sin\frac{\pi}{25}(x - 1.21a t),$$

only for $x = x_{-1}$. Here, we use $a = \sin \theta$. This condition is set up from the solution to Eq. (2) for the case $r = 0$ or $b = 0$ in Eq. (2) and the initial condition Eq. (8), following our analysis in the previous section, the solution is in the form of Eq. (3). Since it is implicit, we use the maximum value for h substituting in f of Eq. (3). The wave changes the form from sinusoidal into a sharp shape for the profile with a negative slope, tends to almost a shock, and appears as a small wave at the crest, similar to what was presented in the previous part. Meanwhile, we also see a decrease in the amplitude with increasing time. This is the effect of the second derivative in Eq. (2). For clearer results, we present the calculation for $h(x, 500)$ in Fig. 2 (b).

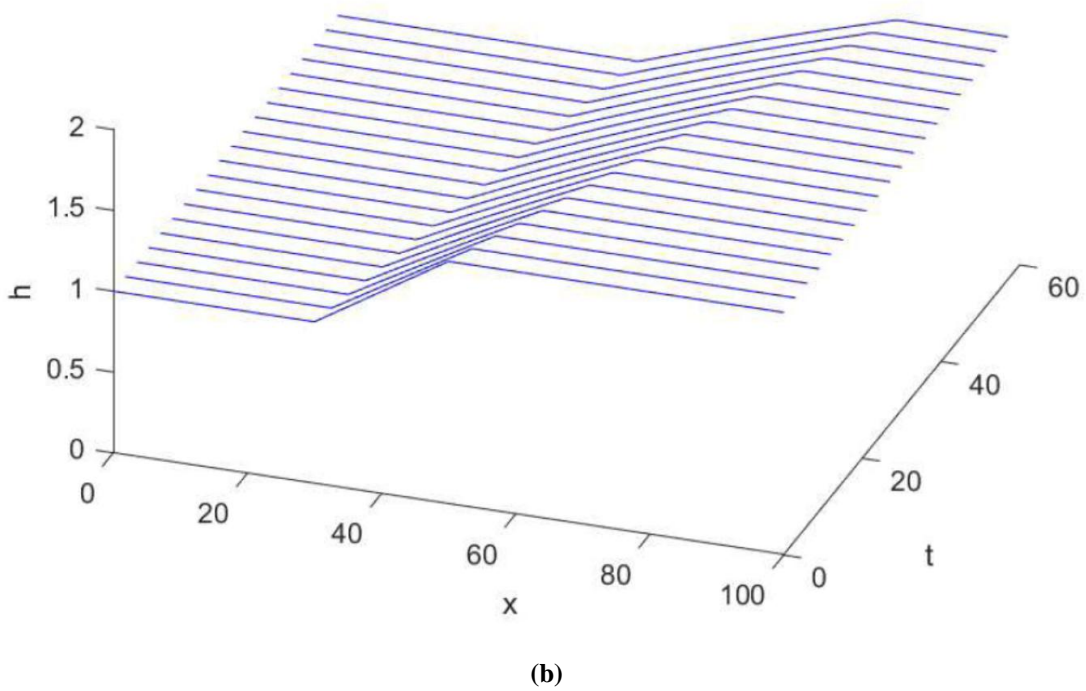
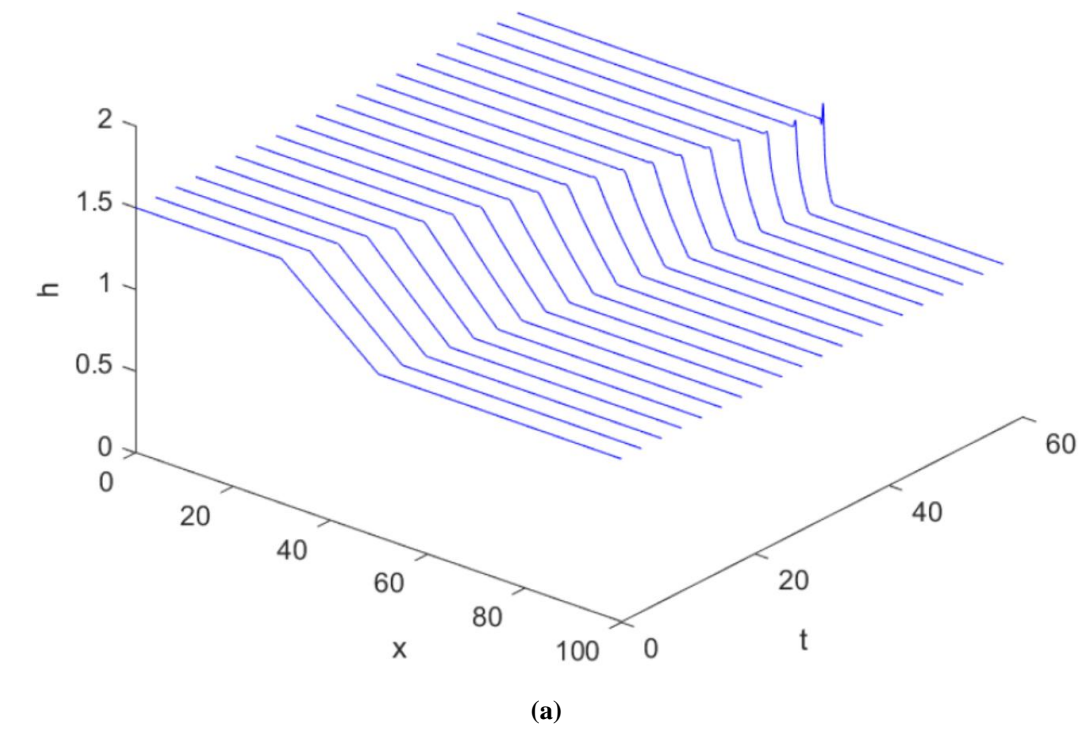
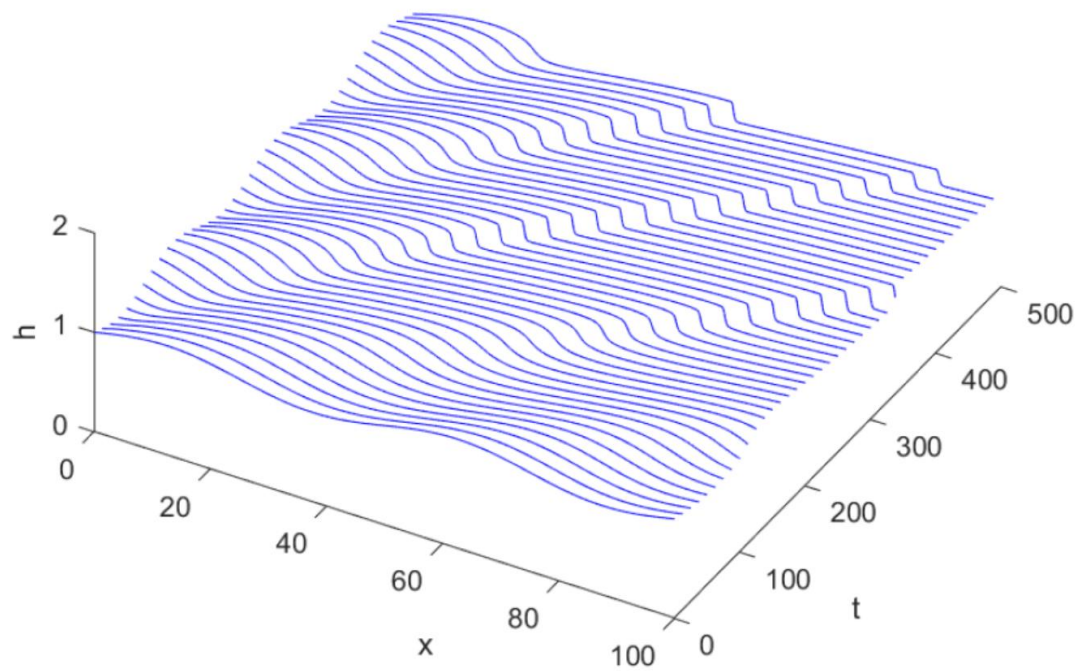
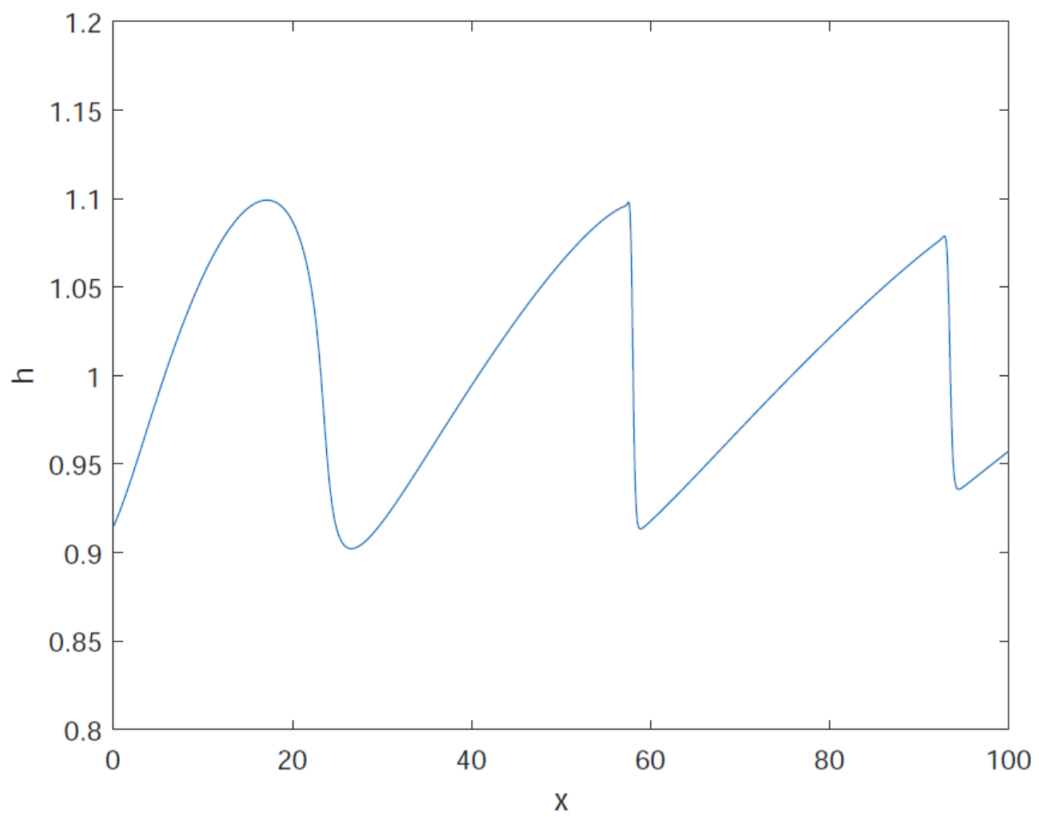


Figure 1. Wave Animation: (a) With Shock, (b) No Shock



(a)



(b)

Figure 2. Simulation Results: (a) Animation $h(x, t)$ of Solution to Eq. (2), (b) Plot $h(x, 500)$

In comparing the parameter r we give a simulation for an incoming wave in the observation domain as the boundary condition

$$h(x, t) = 1 + 0.15 \operatorname{sech}^2 0.3(x + 10 - 3.9 at), \quad (9)$$

only for $x = x_{-1}$ with initial condition $h(x, 0) = 1$. The numerical solution is presented in Fig. 3, calculated using a small value $r = 0.001$ and $\theta = 5^\circ$. This incoming wave propagates with a changing form, reducing the amplitude and sharp shape of the front wave. The second character is mainly due to the effect of the nonlinearity. We can compare this with the linearized model presented in Putra et al. [9], without a sharp shape. The profile of the wave at $t = 350$ is presented in Fig. 4 (a), together with the wave profile for $r = 0.005$ presented in Fig. 4 (b), and $r = 0.01$ presented in Fig. 4 (c). Larger value of r , the wave travels more slowly but reduces the amplitude faster, as the character of the second derivative of Eq. (2) is dominated by a stronger term in that equation. Therefore, we can observe the effect of the inclination θ by considering the value of the coefficient in the second and third terms of Eq. (2), i.e., the value of a and b .

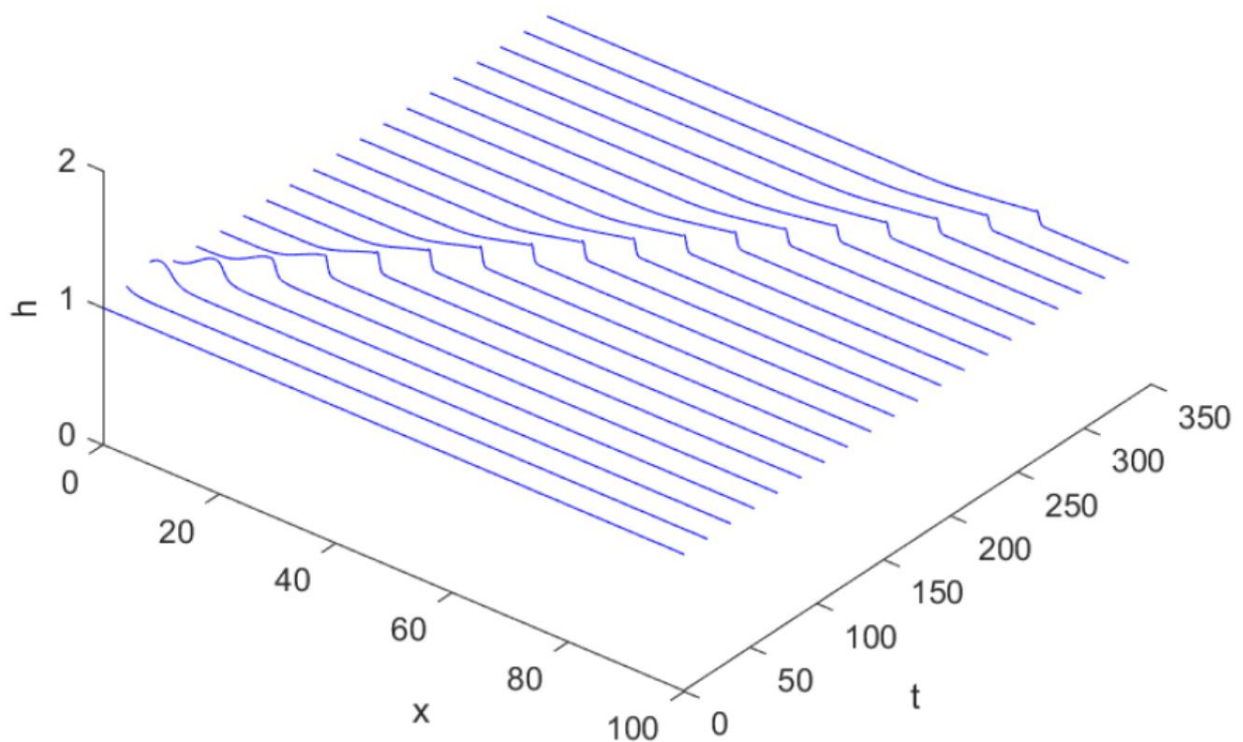
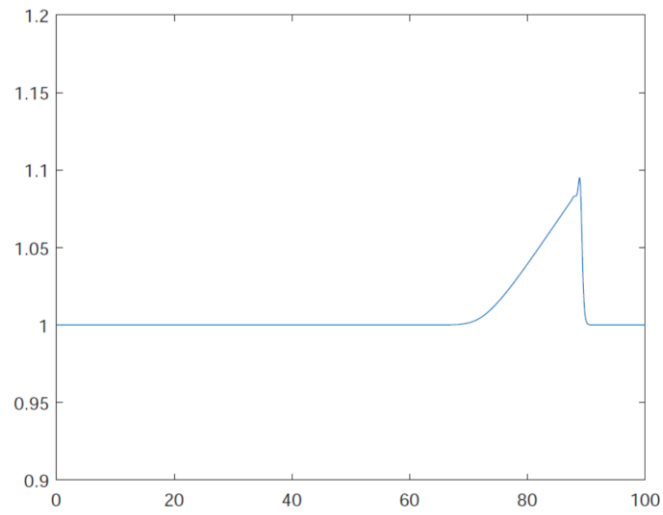
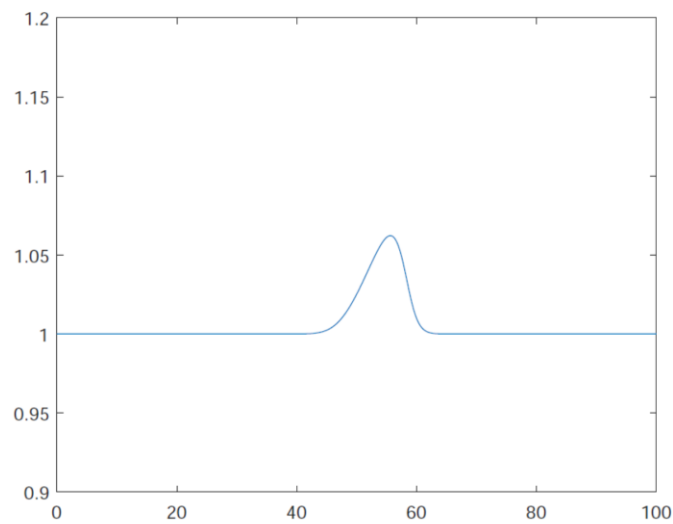


Figure 3. Wave Animation from Incoming Wave on Eq. (9)

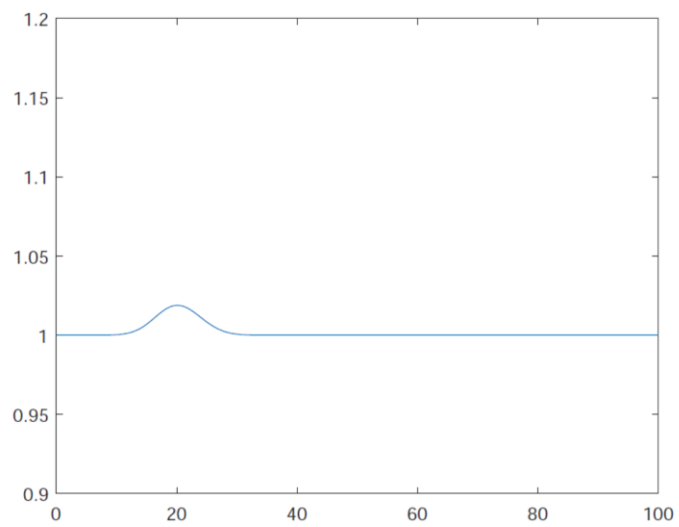
The incoming wave in Eq. (9) is now used to observe the numerical solution of Eq. (2) for different inclinations. The wave propagation is similar to the plot in Fig. 3. For clearer observations, we present the plot of h at a certain time t for different θ . So, we give plot $h(x, 150)$ in Fig. 5 (a) for $\theta = 5^\circ$ and in Fig. 5 (b) for $\theta = 10^\circ$, both calculated using $r = 0.002$. Plot $h(x, 150)$ from $\theta = 10^\circ$ travels faster and fatter waves compared to $\theta = 5^\circ$. We can see that plot for $\theta = 5^\circ$ is sharp in front but without a crest, as it requires more time to run the calculation. Extra time can be given by using different r . This is shown in Fig. 6 (a) as the result of the calculation using $r = 0.001$, $\theta = 5^\circ$. In Fig. 6 (b), we show the result of our calculation using $r = 0.002$, $\theta = 10^\circ$. Both show a similar profile, sharp in front and crest on the top of the wave.



(a)



(b)



(c)

Figure 4. Plot $h(x, 350)$ for Different r where Horizontal Axis is Space x and Vertical Axis is h :
(a) $r = 0.001$, (b) $r = 0.005$, (c) $r = 0.01$

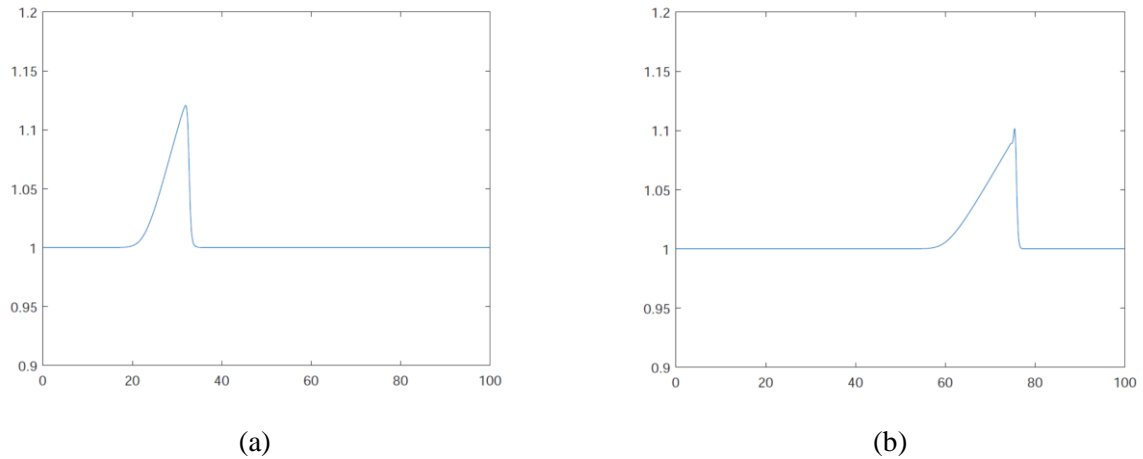


Figure 5. Plot $h(x, 150)$ for Different θ where Horizontal Axis is Space x and Vertical Axis is h :
(a) $\theta = 5^\circ$, (b) $\theta = 10^\circ$

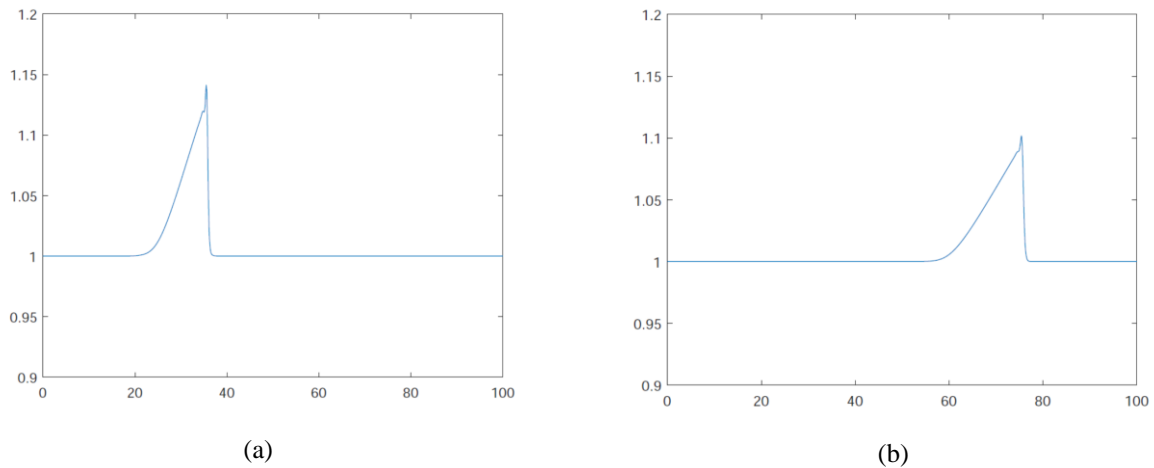


Figure 6. Plot $h(x, 150)$ for Different θ and r where Horizontal Axis is Space x and Vertical Axis is h :
(a) $\theta = 5^\circ, r = 0.001$, (b) $\theta = 10^\circ, r = 0.002$

4. CONCLUSION

A fully nonlinear model of thin film flow on an inclined wall is investigated through numerical simulations. The proposed approach employs an implicit finite difference scheme based on Taylor polynomial approximations, providing stable and accurate solutions for the nonlinear governing equations. The effects of nonlinearity are clearly observed through the progressive steepening of the wave profile, ultimately leading to shock formation. This behaviour is characterised by the transformation of an initially smooth wave with a negative slope into a sharply defined front and crest. The resulting wave structure can be effectively captured by applying an appropriate scaling of the horizontal and vertical axes with respect to time. The present study is limited to numerical experiments on a nonlinear thin film flow model without surface tension, with simulations intentionally terminated prior to the onset of shock formation. Future work will focus on experimental validation through laboratory studies, the incorporation of surface tension effects into the nonlinear model, and the development of advanced numerical techniques capable of accurately resolving shock propagation in nonlinear wave systems.

Author Contributions

Leo Hari Wiryanto: Conceptualization, Data Curation, Software, Writing-Original Draft. Sudi Mungkasi: Methodology, Validation, Visualization, Writing-Review and Editing. Ikha Magdalena: Formal Analysis,

Investigation, Project Administration, Resources. All authors discussed the results and contributed to the final manuscript.

Funding Statement

The research received no specific grant from any funding agency in the public, commercial, or not-for-profit sectors. However, it was the authors' initial work to obtain a research grant from the Ministry of Higher Education, Science, and Technology of the Republic of Indonesia in 2026.

Acknowledgment

The authors thank the editors and the reviewers for their comments and suggestions, which led to the improvement of this paper. The authors also thank the Research Group of Financial and Industrial Mathematics, Institut Teknologi Bandung, and the Department of Mathematics, Sanata Dharma University for supporting this research collaboration.

Declarations

The authors declare no competing interests.

Declaration of Generative AI and AI-Assisted Technologies

The authors declare that no generative AI or AI-assisted technologies were used in the preparation of this manuscript, including writing, editing, data analysis, or the creation of tables and figures.

REFERENCES

- [1] L.H. Wiryanto, "FLOW ON AN INCLINED OPEN CHANNEL," *Nonlinear Analysis and Differential Equations*, vol. 4, no. 11, pp. 541-547, 2016. doi: <https://doi.org/10.12988/nade.2016.6757>
- [2] L.K. Budiasih and L.H. Wiryanto, "ON A STUDY OF STAGGERED LEAPFROG SCHEME FOR LINEAR SWE," *Advances in Mathematics: Scientific Journal*, vol. 9, no.11, pp. 9787-9795, 2020. doi: <https://doi.org/10.37418/amsj.9.11.88>
- [3] R. Fauzi and L.H. Wiryanto, "MOMENTUM CONSERVATIVE SCHEME FOR SIMULATING GRANULAR LANDSLIDE OVER AN INCLINED RIGID BED," *Advances and Applications in Fluid Mechanics*, vol. 27, no. 1, pp. 37-45, 2021. doi: <https://doi.org/10.17654/FM027010037>
- [4] L.H. Wiryanto and M. Jamhuri, "SUPERCRITICAL FLOW GENERATING A SOLITARY-LIKE WAVE ABOVE A BUMP," *IndoMS Journal on Industrial and Applied Mathematics*, vol. 2, no. 1, pp. 1-8, 2015; https://socs.binus.ac.id/wp-content/uploads/2015/06/Paper-1_Vol_2_Issue_1_Jan_2015.pdf
- [5] I. Magdalena and L.H. Wiryanto, "WAVE GENERATION ON AN INCLINED OPEN CHANNEL WITH A BUMP," *International Journal of GEOMATE*, vol. 19, no. 76, pp. 126-133, 2020. doi: <https://doi.org/10.21660/2020.76.42744>
- [6] M.V. Dyke, *PERTURBATION METHOD IN FLUID MECHANICS*, New York, Academic Press, 1964.
- [7] D.J. Acheson, *ELEMENTARY FLUID DYNAMICS*, Oxford, Oxford University Press, 1990. doi: <https://doi.org/10.1093/oso/9780198596608.001.0001>
- [8] C. Pozrikidis, *Fluid Dynamics: Theory, COMPUTATION, AND NUMERICAL SIMULATION*, Boston, Kluwer Academic Publishers, 2009. doi: <https://doi.org/10.1007/978-0-387-95871-2>
- [9] C. King, E.O. Tuck, and J.-M. Vanden-Broeck, "AIR BLOWN ON THIN VISCOUS SHEET," *Physics of Fluids A: Fluid Dynamics*, vol. 5, no. 4, pp. 973-978, 1993. doi: <https://doi.org/10.1063/1.858641>
- [10] A. Oron and P. Rosenau, "FORMATION OF PATTERNS INDUCED BY THERMOCAPILLARY AND GRAVITY," *Journal de Physique II*, vol. 2, no. 2, pp. 131-146, 1992. doi: <https://doi.org/10.1051/jp2:1992119>
- [11] F.F. Abdelall, S.I. Abdel-Khalik, D.L. Sadowski, S. Shin, and M. Yoda, "ON THE RAYLEIGH-TAYLOR INSTABILITY FOR CONFINED LIQUID FILM WITH INJECTION THE BOUNDARY SURFACES," *International Journal of Heat and Mass Transfer*, vol. 49, no. 7-8, pp. 1529-1546, 2006. doi: <https://doi.org/10.1016/j.ijheatmasstransfer.2005.07.055>
- [12] S. Kallianasis, C. Ruyer-Quil, B. Scheid, and M.G. Valarde, *FALLING LIQUID FILMS*, London, Springer, 2012. doi: <https://doi.org/10.1007/978-1-84882-367-9>.
- [13] L.H. Wiryanto and W. Febrianti, "NUMERICAL SOLUTION OF THIN-FILM FLOWING DOWN ON AN INCLINED CHANNEL," *Advances and Applications in Fluid Mechanics*, vol. 20, no. 4, pp. 595-604, 2017. doi: <https://doi.org/10.17654/FM020040595>

- [14] L.H. Wiryanto, "A FINITE DIFFERENCE METHOD FOR A THIN FILM MODEL," *Proceedings of International Conference on Mechanical, Electrical and Medical Intelligent System 2017 (ICMEMIS2017)*, GS-02; <http://www.e-jikei.org/Conf/ICMEMIS2017>
- [15] L.H. Wiryanto, "STABILITY ANALYSIS OF THIN FILM MODEL," *Journal of Physics: Conference Series*, vol. 983, no. 1, art. 012072, 2018. doi: <https://doi.org/10.1088/1742-6596/983/1/012072>
- [16] L.H. Wiryanto, R. Widayawati, R. Fauzi, G. Putra, and E. Noviani, "SIMULATION OF WAVE PROPAGATION ON THIN FILM," *Advances and Applications in Fluid Mechanics*, vol. 29, pp. 45-58, 2022. doi: <https://doi.org/10.17654/0973468622007>
- [17] G. Putra, L.H. Wiryanto, and R. Widayawati, "AN IMPLICIT FINITE DIFFERENCE METHOD FOR THIN FILM FLOW," *Journal of the Indonesian Mathematical Society*, vol. 29, no. 1, pp. 99-105, 2023. doi: <https://doi.org/10.22342/jims.29.1.1110.99-105>
- [18] L.H. Wiryanto and W. Djohan, "FOURTH ORDER PDE MODEL OF THIN FILM FLOW INVOLVING SURFACE TENSION," *Journal of the Indonesian Mathematical Society*, vol. 31, no. 2, pp. 1-10, 2025. doi: <https://doi.org/10.22342/jims.v31i2.1454>
- [19] L.H. Wiryanto and A. Achirul, "AN IMPLICIT FINITE DIFFERENCE METHOD FOR A FORCED KDV EQUATION," *Jurnal Matematika*, vol. 11, no. 1, pp. 1-5, 2008; <https://ejournal.undip.ac.id/index.php/matematika/article/view/386>
- [20] L.H. Wiryanto, "NUMERICAL SOLUTION OF A KDV EQUATION, MODEL OF A FREE SURFACE FLOW," *Applied Mathematical Sciences*, vol. 8, no. 93, pp. 4645-4653, 2014. doi: <https://doi.org/10.12988/ams.2014.46404>
- [21] L.H. Wiryanto, "A FINITE DIFFERENCE METHOD FOR KDV EQUATION AS THE MODEL OF INTERFACIAL WAVE," *Advances and Applications in Fluid Mechanics*, vol. 23, no. 2, pp. 161-169, 2019. doi: <https://doi.org/10.17654/FM023020161>
- [22] W. Rohlfis and P. Pischke, "HYDRODYNAMIC WAVES IN FILM FLOWING UNDER AN INCLINED PLANE," *Physical Review Fluids*, vol. 2, art. 044003, 2017. doi: <https://doi.org/10.1103/PhysRevFluids.2.044003>
- [23] R. Fauzi and L.H. Wiryanto, "ON THE STAGGERED SCHEME FOR SHALLOW WATER MODEL DOWN AN INCLINED CHANNEL," *AIP Conference Proceedings*, vol. 1867, no. 1, 2017. doi: <https://doi.org/10.1063/1.4994405>
- [24] R. Fauzi and L.H. Wiryanto, "PREDICTOR-CORRECTOR SCHEME FOR SIMULATING WAVE PROPAGATIONAL SHALLOW WATER REGION," *IOP Conference Series: Earth and Environmental Science*, vol. 162, no. 1, art. 012047, 2018. doi: <https://doi.org/10.1088/1755-1315/162/1/012047>
- [25] D.J. Needham and J.H. Merkin, "ON ROLL WAVES DOWN AN OPEN INCLINED CHANNEL," *Proceedings of the Royal Society of London. A. Mathematical and Physical Sciences*, vol. 394, no. 1807, pp. 259-278, 1984. doi: <https://doi.org/10.1098/rspa.1984.0079>
- [26] J.H. Merkin and D.J. Needham, "AN INFINITE PERIODIC BIFURCATION ARISING IN ROLL WAVES DOWN AN OPEN INCLINED CHANNEL," *Proceedings of the Royal Society of London. A. Mathematical and Physical Sciences*, vol. 405, no. 1828, pp. 103-116, 1986. doi: <https://doi.org/10.1098/rspa.1986.0043>
- [27] R.F. Dressler, "MATHEMATICAL SOLUTION OF THE PROBLEM OF ROLL-WAVES IN INCLINED OPEN CHANNELS," *Communications on Pure and Applied Mathematics*, vol. 2, no. 2-3, pp. 149-194, 1949. doi: <https://doi.org/10.1002/cpa.3160020203>
- [28] L.H. Wiryanto, "THIN FILM FLOW ON AN INCLINED CHANNEL," *Proceedings of International Conference on Technology and Social Science 2018 (ICTSS 2018)*, A010; <https://conf.e-jikei.org/ICTSS2018>
- [29] L.H. Wiryanto, "THIN FILM FLOW OVER A BUMP ON AN INCLINED CHANNEL," *Journal of Physics: Conference Series*, vol. 1321, no. 2, art. 022058, 2019. doi: <https://doi.org/10.1088/1742-6596/1321/2/022058>
- [30] W.A. Strauss, *PARTIAL DIFFERENTIAL EQUATION: AN INTRODUCTION*, Hoboken, John Wiley & Sons, 2008.